IRSTI 44.37.29 10.26577/ijmph.202617113

MATHEMATICAL MODEL OF COGENERATION ENERGY COMPLEX WITH SOLAR RADIATION CONCENTRATION

P. Nesterenkov [1], **L. Nesterenkova** [1], **A. Temirbekov** [1], **A. Nesterenkov** [1] **and S. Starukhin** [1]

[1] *Farabi University, Almaty, Kazakhstan*

Email: stolkner@gmail.com

(Received 11 September 2024; revised 22 December 2025; accepted 10 March 2026)

Abstract. Based on the results of testing linear photovoltaic modules (Λ-PM) with optical concentrators, as well as studies on heat transfer in channels with heat-generating photovoltaic cells on the walls, a new type of equipment has been developed — an energy complex with Λ-PM and a cooling system. In this system, the technological contradiction caused by the decrease in the electrical efficiency of silicon photovoltaic cells with increasing outlet water temperature is reduced. To achieve this, half of the photovoltaic cells operate at a relatively low temperature ($< 40^{\circ}$C) to maintain sufficient efficiency, while the other half work at a high temperature ($\approx 70^{\circ}$C), generating, in addition to electricity, high-potential thermal energy. As a result, the total performance in terms of electricity and heat equals the overall performance of a standard PM with the same concentrator aperture area, moreover, high-potential heat is produced for hot water supply. A mathematical model and a methodology for calculating the output characteristics of the energy complex are presented, based on the thermal energy balance in the Λ-PM channels with mutual shielding of thermal radiation from the frontal walls. Using a Python-based software application, iterative calculations of water temperature and flow rate, as well as the specific electrical and thermal power of the energy complex, were performed.The results demonstrate a significant advantage of the developed cogeneration technology compared to known analogues. Through numerical experimentation, the reliable removal of heat from the surface of Maxeon-type silicon photovoltaic cells under natural water circulation in the cooling system in the laminar viscous-gravitational flow regime was demonstrated. With the help of the software application, computer simulations were carried out to forecast the performance of the energy complex in regions with different solar resources.

Keywords: linear photovoltaic module, optical concentrator, cooling system, circulation loop, heat transfer coefficient, mathematical model, thermal efficiency

INTRODUCTION

A key drawback of cogeneration is the internal contradiction arising from the decrease in electrical efficiency of photovoltaic cells as the output water temperature in the storage system increases. This work presents a technical solution to address this technological shortcoming and describes a mathematical model for a technology where photovoltaic cells maintain high electrical efficiency while generating high-potential thermal energy in the form of hot water. The technological scheme and operating principle of a prototype energy complex with low- and high- temperature Λ–PMs and an innovative cooling system with natural water circulation in the storage system are presented. A Python-based software application has been developed for calculations, and the results of the specific performance calculations for the energy complex are discussed.

LITERATURE REVIEW

In the pilot installation with high solar radiation concentration (SR), electricity generation and high-potential heat in the form of hot water were achieved using high-temperature solar cells based on GaAs and a heat exchanger with a high-pressure heat transfer fluid [1, 2]. The high specific heat flux from the surface of the photovoltaic cells was achieved by reducing the thermal resistance from the previous technical level of approximately 0.5 $cm^2 K/W$ to about 0.09 $cm^2 K/W$. This was accomplished by creating microchan-

nels in a ceramic substrate made of silicon carbide (SiC), onto which GaAs-based elements were soldered in a vacuum. The drawbacks of such installations include the complexity of manufacturing optical concentrators and cooling devices, the need for precision solar tracking systems, and consequently, high costs.

In the field of large-scale electricity and heat production, Cogenra Solar installations with linear PMs using silicon photovoltaic cells of relatively large area are more promising for efficiently extracting the generated heat [3]. Each module is 2.5 meters long, and the parabolic concentrator, equipped with 12 flat mirrors and approximately 3 meters wide, is controlled using the SunDeck software application. With an eightfold optical concentration of solar radiation at the latitude of South Carolina (USA), the peak specific power for electricity is approximately 100 $\mathrm{W/m^2}$ and for heat is approximately 560 $\mathrm{W/m^2}$. Testing of the installation showed a 4.7-fold increase in total (electrical + thermal) energy $(168+657)$ $\mathrm{kWh/m^2}$ compared to standard photovoltaic panels of the same aperture.

Stylianou [4] presents the methodology and results of calculating heat transfer in the water channels of the Cogenra Solar installation using Ansys Fluent for laminar flow cases, where the Navier–Stokes equations can be solved numerically. The drawbacks of these installations include significant optical and thermal losses, substantial energy costs for pump operation, and a high specific cost of approximately $\$1460/\mathrm{m^2}$.

In studies of linear PMs with up to 30 sun concentration, electrical efficiency of approximately 0.11 and thermal efficiency of approximately 0.57 have been achieved, highlighting the importance of uniform illumination across the photovoltaic array [5]. Shadows cast by the mounting supports of trough concentrators reduced electrical performance by about 7%. One solution to this problem is to use stationary PMs and eliminate the shading supports.

Results from Xu Ji et al. [6] describe a system with a concentrator and a north-to-south oriented linear PM, 0.12 meters wide and 1.5 meters long. With a geometric concentration of approximately 17 and a mirror reflectivity of 0.69, the optical concentration reached about 10.3. Silicon photovoltaic cells were affixed using a thermal conductive tape to a cooling plate of the channel, which had an internal diameter of 0.03 meters. The one-dimensional steady-state heat transfer mathematical model assumed constant wall temperatures and considered the average logarithmic temperature gradient between the wall and the water flow.

In systems with concentrators, optical losses occur due to light reflection on the surfaces of mirrors and through protective glass. Additionally, the radiation that reaches the photovoltaic cells is partially reflected through the glass into the space, resulting in additional losses of about 1%. Bernardo et al. [7] provide the transmission coefficient for light through thick protective glass $k_0 \approx 0.90$ with the light reflection coefficient on its surfaces $\xi_0 \approx 0.08$ and the absorption coefficient in the glass of approximately 0.02.

Recent studies [8, 9] also confirm the growing interest in solar thermal systems and mathematical modeling of heat-transfer processes. In particular, the work devoted to solar-assisted autocascade heat pumps for water heating in continental climates demonstrates the effectiveness of combined solar thermal technologies for autonomous energy supply systems and emphasizes the importance of thermal regime optimization under varying climatic conditions. In addition, [10] investigated an inverse problem for determining coefficients in the heat conduction equation, highlighting the significance of mathematical methods for accurate modeling of heat-transfer processes in energy systems. These studies provide an important theoretical and applied basis for the development of the present mathematical model of a cogeneration energy complex with concentrated solar radiation.

Materials and Methods

To reduce optical and thermal losses, a design with Λ-shaped cross-sectional flat channels has been developed. Figure 1 illustrates an innovative Λ-PM with flat channels made of aluminum

alloy, installed at an angle of 2φ. In this design, the reflection coefficient is reduced to $\xi_0 \approx 0.06$, eliminating the need for thick protective glass on the front walls, while mechanical damage during cleaning is prevented by a polytetrafluoroethylene (lavsan) film. Part of the radiation reflected from the protective glass is lost to the surrounding space, but about 9% returns to the photovoltaic cells on the opposite wall. As a result, the Λ-shaped PM receives the total radiation:

$$\begin{aligned}&\left(1-(\xi_0+k_{\text{p}})\right)\cdot C_{\text{or}}\cdot I_m\\&\quad+0.09\cdot\xi_0\cdot C_{\text{or}}\cdot I_m\approx 0.94\cdot C_{\text{or}}\cdot I_m\end{aligned}$$

where:

- I_m — intensity of light;
- C_{or} — concentration of light.

Consequently, the total transmission coefficient in the Λ-PM increases by a factor of $(1+0.15\cdot\xi_0)$ and reaches: $k_0 \approx 0.91\cdot(1+0.15\cdot\xi_0)\approx 0.92$.

The counter-placed front walls of the channels, due to mutual shielding, reduce thermal radiation losses by approximately 27% compared to Λ-shaped PM. Additionally, the inverted channel creates a thermal cushion inside, with a temperature higher than the surrounding environment, which also reduces convective heat losses. Together, these factors contribute to obtaining high-potential thermal energy.

According to Luque [11], peak specific electrical power generated by an array of silicon photovoltaic cells is determined from the expression:

$$\begin{aligned}P=k_0\cdot I_m\cdot C_{\text{op}}\cdot\eta_{e0}\left(1-\frac{0.011\cdot\Delta t_1}{P_0}\right)\\\times\left(1+\frac{k\cdot T}{q\cdot U_{\text{OC}}}\ln\ln C_{\text{op}}\right)\cdot\frac{F'}{F}\end{aligned}\qquad(1)$$

where:

- η_{e0} — efficiency of the photovoltaic cell ≈ 0.22;
- P_0 — power of the photovoltaic cell ≈ 1.1 W;
- U_{OC} — voltage of the photovoltaic cell ≈ 0.64 V;
- $\frac{F'}{F}$ — ratio of fill factors with and without concentration ≈ 0.8;
- S_f — area of the photovoltaic array;
- k — Boltzmann constant, $\text{eV}\cdot\text{K}^{-1}$;
- q — electron charge;
- T — temperature, °C.

The experimental value of the parameter is:

$$\left(1+\frac{k\cdot T}{q\cdot U_{\text{OC}}}\ln\ln C_{\text{op}}\right)\cdot\frac{F'}{F}\approx 0.89.$$

With a width of the front walls of 0.186 m and a focal length to the concentrator mirrors of 3 m, the average cosine of the mirror angles is 0.91. Therefore, for 12 mirrors with a width of 0.19 m, the geometric concentration is: $K_g \approx \frac{2.07}{0.185}\approx 11.2$.

The reflection coefficient for the mirror film Alanod Miro Sun is approximately 0.93. Thus, the optical coefficient is: $C_{\text{op}}\approx 0.93\cdot 0.91\cdot 11.2\approx 9.4$.

Substituting these numerical values into equation(1), we obtain:

$$P=7.8\cdot I_m\cdot\eta_e\qquad(2)$$

According to the law of energy conservation, useful peak specific thermal power transferred to the water is determined by the expression:

$$Q=8.8\cdot I_m\left(1-\frac{S_f}{S_Q}\cdot 0.89\cdot\eta_e\right)-1.5\cdot q_\Lambda,\quad(3)$$

where:

- S_Q — area of the front walls, m^2;
- q_Λ — specific thermal losses to the environment (with a numerical factor of 1.5 accounting for heat losses through the front and side surfaces of the channels).

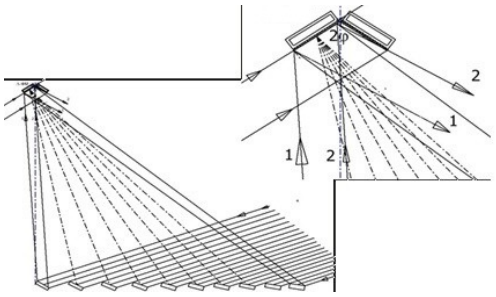

Figure 1 - Λ-PM and the direction of optical flows

For Maxeon type A photovoltaic cells, $\frac{S_f}{S_Q} \approx 0.83$.

According to the patented technology [**?**], temperature of the photovoltaic cells in the low-temperature Λ-PM is stabilized at

$$t_{f1} \leq 40^{\circ}\text{C},$$

while temperature of the photovoltaic cells in the other Λ-PM increases to

$$t_{f2} \approx 70^{\circ}\text{C},$$

through multiple circulations of water along the flat channel contour, storage tank, and return pipeline. For low- and high-temperature photovoltaic arrays with areas

$$S_{f1} = S_A \cdot (2n+10)$$

and

$$S_{f2} = S_A \cdot (2n+34),$$

the sum of the peak electrical power is:

$$P_1 + P_2 \approx 7.8 \cdot I_m \left(S_{f1} \cdot \eta_{e1} + S_{f2} \cdot \eta_{e2}\right).$$

V-shaped linear PMs with the same area of photoelements

$$S_{f3} = 2 \cdot S_A \cdot (2n+22)$$

at a temperature

$$t_{f\text{avg}} \approx \frac{t_{f1}+t_{f2}}{2} \approx 55^{\circ}\text{C}$$

produce power:

$$P_3 \approx 7.8 \cdot I_m \cdot 2 \cdot S_{f3} \cdot \eta_{e3}.$$

Thus, the value of the ratio is:

$$\frac{P_1+P_2}{P_3} \approx \frac{(2n+10)\cdot 0.85 + (2n+34)\cdot 0.55}{2\cdot(2n+22)\cdot 0.7} \approx 1.$$

For the areas of the front panels:

$$S_{Q1} = (0.042 \cdot 0.15) \cdot (2n+10) \approx 1.39 \text{ m}^2$$

and

$$S_{Q2} = (0.042 \cdot 0.15) \cdot (2n+34) \approx 1.54 \text{ m}^2,$$

the total useful thermal power is:

$$Q_1 + Q_2 \approx [12.3 \cdot I_m \cdot 0.86 - 2.1 \cdot q_{\Lambda 1}] + [13.7 \cdot I_m \cdot 0.91 - 2.3 \cdot q_{\Lambda 2}].$$

For standard PMs with the same total panel area

$$S_{Q3} \approx 2.93 \text{ m}^2,$$

total useful thermal power is:

$$Q_3 \approx [26.0 \cdot I_m \cdot 0.89 - 4.4 \cdot q_{\Lambda 3}].$$

The specific thermal losses due to radiation and convection, considering the mutual shielding of thermal radiation from the panels, with

$$\xi \approx 0.27,$$

are determined from the expression:

$$q_\Lambda = \frac{t_f - t_0}{R_2} + (1-\xi) \cdot \frac{t_f - t_0}{R_r}, \qquad (4)$$

where:

- R_2 — thermal resistance due to air convection, $\approx 0.19 \text{ m}^2 \cdot \text{K/W}$.

$$R_r \approx \left[0.04 \cdot \varepsilon \cdot \sigma_0 \left(\frac{t_f + t_0}{200} + 2.73\right)^3\right]^{-1}$$

where:

- ε — emissivity of the wall, ≈ 0.8;
- σ_0 — Stefan–Boltzmann constant for a black body, ≈ 5.67 W$/(\mathrm{m}^2 \cdot \mathrm{K}^4)$;
- t_0 — ambient temperature, °C.

In the operating temperature ranges

$$t_{f1} \approx (40-5)^\circ\mathrm{C}$$

and

$$t_{f2} \approx (70+5)^\circ\mathrm{C},$$

the following equality holds:

$$(q_{\Lambda 1} + q_{\Lambda 2}) \approx 2 \cdot q_{\Lambda 3},$$

from this, we get:

$$\frac{Q_1 + Q_2}{Q_3} \approx \frac{[10.9 \cdot I_m - 2.1 \cdot q_{\Lambda 1}]}{23.4 \cdot I_m - 4.4 \cdot q_{\Lambda 3}} + \frac{[12.5 \cdot I_m - 2.3 \cdot q_{\Lambda 2}]}{23.4 \cdot I_m - 4.4 \cdot q_{\Lambda 3}} \approx 1.$$

Numerical calculations show that adjacent low- and high-temperature Λ-PM produce the same total amount of electrical and thermal energy as a pair of identical PMs. Additionally, they provide high-potential thermal energy in the form of hot water with a temperature above 60°C and transport it to the storage system using natural circulation, i.e., without pumps. The fivefold excess of thermal energy over electrical energy promotes the development of associated businesses when placed within metal structures of energy complexes, such as greenhouses or pellet drying devices. Figure 2 shows a prototype of an energy complex with concentrators placed on different sides of the support structure. The cooling system for low- and high-temperature Λ-PMs includes: flat channels of length L installed at an angle ε to the horizontal; receiving and storage tanks with a height h; return pipelines with a height

$$H \approx (L\varepsilon - h);$$

heat exchangers in the form of axisymmetric annular channels running along the return pipelines and connecting the cold source with the receiving tanks; and supply pumps that deliver water from the source. Under the effect of thermosiphon, water rises through the flat channels into the receiving tank and, mixing with the incoming water, flows into the return pipeline. The cooling properties of the water are restored through heat exchange with the incoming water supplied by the pump through the annular channels. As a result, the temperature at the inlet of the low-temperature Λ-PM channels is maintained at around ≈ 17°C. After the receiving tank is filled, hot water from the upper level flows by gravity into the main storage tank. A similar process occurs in the high-temperature circuit, with the only difference being that the pump for the incoming water operates significantly less frequently. Water has a unique combination of thermophysical properties that automatically shifts the process to a lower temperature level during heat exchange. Figure **??** depicts graphs showing the rate of decrease in the density and viscosity of water within the working temperature range. This creates a negative feedback loop that moves the water mass to a more favorable temperature level and, consequently, to a higher heat transfer coefficient. The heat released by the photovoltaic elements increases the enthalpy of the water and performs work to transport it to a height of about four meters. During the night, the potential energy of the water is released in the process of providing hot water to consumers. To obtain the mathematical model of the process, let us denote the average temperature, density, and viscosity of the water in the flat channels and receiving tank as t, ρ, ν and t_h, ρ_h respectively; the temperature, density, and viscosity in the return pipeline as t_{tr}, ρ_{tr}, ν_{tr} respectively. The diameter of the return pipeline is

$$d_{\mathrm{tr}} \approx 3d,$$

the length of the pipeline is

$$L_{\mathrm{tr}} \approx 2L,$$

and the coefficient of local resistances does not

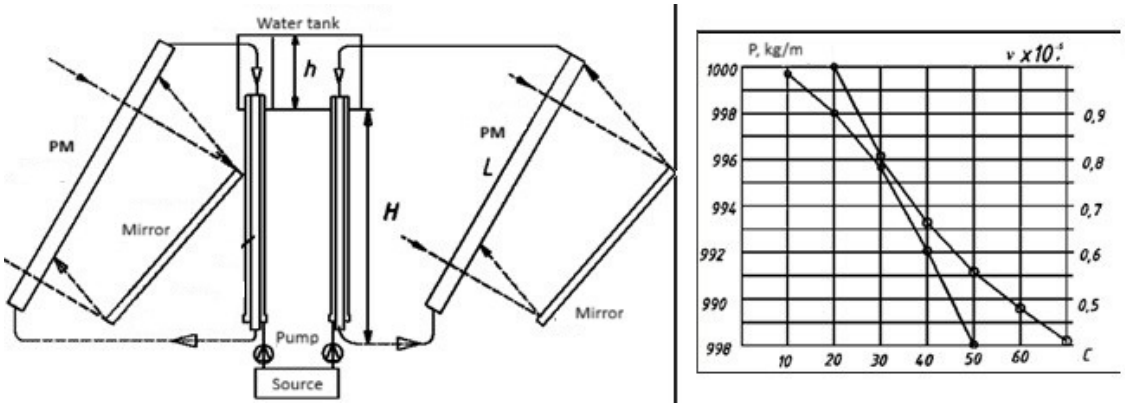

Figure 2 - Water circulation diagram with explanatory graphs

exceed

$$\zeta \leq 5.$$

The flow velocity of the water in the return pipeline is found using the continuity equation in a closed loop:

$$\frac{\pi d^2}{4}\rho u = \frac{\pi (3d)^2}{4}\rho_{\text{tr}} u_{\text{tr}},$$

from this, we get:

$$u_{\text{tr}} = 0.22u\frac{\rho}{\rho_{\text{tr}}}.$$

The physical cause of natural circulation is the difference in the weight of water columns in the communicating branches of the closed circulation loop [12]. When the total weight of the water column in the receiving tank and the vertical part of the return pipeline exceeds the weight of the water column in the flat channels, natural circulation occurs due to the dynamic pressure:

$$\Delta P \approx g\rho\left[(H+\Delta h)\left(\frac{\rho_{\text{tr}}}{\rho}-1\right) + (h-\Delta h)\left(\frac{\rho_h}{\rho}-1\right)\right].$$

The pressure head is used to compensate for the hydraulic resistance due to friction during water flow in the flat channels and return pipeline (the first two terms in the equation) and to compensate for local resistances due to bends and constrictions in the water flow:

$$2\cdot\frac{64}{Re}\cdot\frac{\rho u^2}{2}\cdot\frac{L}{d}+\frac{64}{Re_{\text{tr}}}\cdot\frac{\rho_{\text{tr}}u_{\text{tr}}^2}{2}\cdot\frac{L_{\text{tr}}}{3d} \cdot\left[(\sin\varepsilon+\cos\varepsilon)-\frac{h}{L}\right]+\zeta\cdot\frac{\rho u^2}{2}=\Delta P.$$

From the balance of forces, we derive the equation of motion for water in the circulation loop:

$$u^2+\frac{26L\nu}{d^2}\left(1+0.03\frac{\nu_{\text{tr}}}{\nu}\right)u -(3.5L+0.4)\left(\frac{\rho_{\text{tr}}}{\rho}-1\right)-3.5\left(\frac{\rho_h}{\rho}-1\right)=0. \tag{5}$$

From this, we find the flow velocity in flat channels:

$$u=-\frac{A_1}{2}+\sqrt{\frac{A_1^2}{4}-B_1}.$$

where

$$A_1=\frac{26L\nu}{d^2}\left(1+0.03\frac{\nu_{\text{tr}}}{\nu}\right),$$

$$B_1=-(3.5L+0.4)\left(\frac{\rho_{\text{tr}}}{\rho}-1\right)-3.5\left(\frac{\rho_h}{\rho}-1\right).$$

Flat channels with a height $\delta \approx 0.008$ m have six longitudinal reinforcing ribs with a thickness of 0.002 m. Therefore, the internal cross-section of the channels is:

$$S_Q \approx 2\delta\,(b-6\cdot 0.002).$$

The water flow rate through them is determined by the expression:

$$\dot{m} \approx 2\delta\,(b - 6\cdot 0.002)\,\rho u \cdot 3600 \approx 7.9\rho u \quad \text{kg/h}.$$

Due to the spatial overlap of the outflowing water streams from the receiving tank and the annular channel, an additional heat balance equation has been introduced:

$$(t - t_x)\,\dot{m}_x = -\,(t_{\text{in}} - t)\,\dot{m}, \tag{6}$$

obtaining the missing expression for the inlet temperature:

$$t = \frac{t_{\text{in}} - (\dot{m}_x/\dot{m})\,t_x}{1 - \dot{m}_x/\dot{m}}.$$

The parameter value varies in the range

$$\dot{m}_x/\dot{m} \approx 0.2\text{–}0.5$$

by periodically switching on pumps to supply cold water. The cogeneration process is considered within the framework of the classical problem of steady-state heat transfer in a channel with second-kind boundary conditions on the frontal surface of the wall and third-kind boundary conditions on the inner surface [13]. The heat-generating photovoltaic cells create a constant specific heat flux according to equation (3), with the external walls being adiabatic. In the mathematical model, two real parallel channels Λ-PM are represented by a single virtual channel with an equivalent diameter of approximately

$$d_e \approx 4\delta,$$

in which the thermophysical properties of the water are constant across the cross-section. The one-dimensional differential heat transfer equation for a channel element of length dx is:

$$\frac{dt}{dx} = \frac{[8.8I_m(1 - 0.76\eta_e) - 1.5q_\Lambda]\cdot 2b}{C_p\dot{m}}.$$

where C_p is the specific heat capacity and $\dot{m}$ is the water flow rate. Integrating along the length, we obtain the heat balance equation for determining the temperature and water flow rate:

$$S_Q\,[8.8I_m(1 - 0.76\eta_e) - 1.5q_\Lambda] = 2C_p\dot{m}(t - t_{\text{in}}), \tag{7}$$

where t_{in} is the inlet temperature of the water (°C) and t is the average temperature of the water along the channel length (°C). Thus, we obtained two equations (5) and (7) with two unknowns temperature and water flow rate. By substituting the parameters of the photovoltaic cells, the concentrator, and the climatic data into the equations, the specific output characteristics of the energy complex are calculated using the method of successive approximations. The key question of the technology is whether the water in natural circulation mode will remove the heat generated by the photovoltaic cells, stabilizing the temperature at a level of $\leq 40\,^\circ$C. To answer this question, we conduct a numerical experiment. In heat engineering calculations, the physical properties of water are considered at the average temperature in the channel. The temperature difference between the photovoltaic cells and the channel wall (on the adhesive layers) does not exceed $\Delta t_w < 2\,^\circ$C; therefore, the temperature of the inner surface of the walls is approximately

$$t_w \approx 38\,^\circ\text{C}.$$

During the most heat-stressed summer period, when the ambient temperature is around 35 °C, the specific heat losses, according to equation (4), are

$$q_{L1} = \left[27 + 0.73\cdot(5)\cdot(0.37 + 2.73)^3\right] \approx 50\ \text{W/m}^2,$$

and according to the left-hand side of equation (7), the generated thermal energy at $I_m = 940$ reaches

$$(10.9\cdot I_m - 2.1\cdot 50) \approx 10150\ \text{W}.$$

With an inlet temperature

$$t_{\text{in}} \approx 17\,^\circ\text{C},$$

we use the iteration method to determine the water temperature at which its thermophysical properties maintain such a velocity and flow rate in the channels that the heat balance (7) is satisfied. Taking the first approximation $t \approx 25\,^\circ$C, we obtain an outlet temperature

$$t_{\text{out}} = 2t - t_{\text{in}} \approx 33\,^\circ\text{C},$$

and in the return pipeline, according to equation (6),

$$t_{\text{in}}^{*} = \frac{t_{\text{in}} - \dot{m}_x/\dot{m} \cdot t_x}{1 - \dot{m}_x/\dot{m}} \approx 19\,^{\circ}\text{C}.$$

Therefore, the average temperature in the receiving tank is

$$t_h \approx \frac{t_{\text{out}} + t_{\text{in}}^{*}}{2} \approx 27\,^{\circ}\text{C},$$

and in the return pipeline,

$$t_{\text{tr}} = \frac{t_{\text{in}} + t_{\text{in}}^{*}}{2} \approx 18\,^{\circ}\text{C}.$$

According to the obtained temperatures, the water in the channels has a density

$$\rho \approx 996.95 \text{ kg/m}^3$$

and viscosity

$$\nu \approx 0.893 \times 10^{-6} \text{ m}^2/\text{s},$$

while in the receiving tank

$$\rho_h \approx 996.6 \text{ kg/m}^3,$$

and in the return pipeline

$$\rho_{\text{tr}} \approx 998.4 \text{ kg/m}^3.$$

From equation (5), we find

$$A_1 = 0.432, \qquad B_1 = -0.025,$$

and the velocity

$$u = 0.052 \text{ m/s},$$

from which the water flow rate is obtained:

$$\dot{m}_1 \approx 7.9 \cdot \rho \cdot u = 7.9 \cdot 996.95 \cdot 0.052 \approx 406 \text{ kg/h}.$$

Substituting this into the right-hand side of equation (7), we obtain

$$2C_p \dot{m}_1 (t - t_{\text{in}}) = 2.32 \cdot 406 \cdot (25 - 17) \approx 7530 \text{ W}.$$

It can be seen that the left-hand and right-hand sides of equation (7) do not coincide. Therefore, a second approximation is performed by taking

$$t \approx 26\,^{\circ}\text{C},$$

at which the velocity increases to

$$u \approx 0.06 \text{ m/s},$$

the flow rate becomes

$$\dot{m}_1 \approx 473 \text{ kg/h},$$

and the right-hand side of equation (7) increases to

$$2.32 \cdot 473 \cdot 9 \approx 9880 \text{ W}.$$

Since the balance is still not achieved, the temperature is increased to

$$t \approx 26.3\,^{\circ}\text{C}.$$

In this case, the flow rate becomes

$$\dot{m}_1 \approx 493 \text{ kg/h},$$

and the right-hand side of the equation is

$$2.32 \cdot 493 \cdot 9.3 \approx 10640 \text{ W},$$

which is close to the value on the left-hand side of equation (7). Therefore, the solution may be accepted at

$$t \approx 26.3\,^{\circ}\text{C}, \qquad u \approx 0.063 \text{ m/s}.$$

In this case, the Grashof number is

$$\text{Gr} = \frac{g\beta\Delta t\, d_E^3}{\nu^2} \approx \frac{9.8 \cdot 2.8 \times 10^{-4} \cdot 9.3 \cdot (0.016)^3}{(0.87 \times 10^{-6})^2} \approx 1.3 \times 10^5$$

and the Reynolds number is

$$\text{Re} = \frac{0.063 \cdot 0.016}{0.87 \times 10^{-6}} \approx 1150,$$

which indicates a viscous–gravitational flow regime in the channels.

The heat transfer coefficient is determined from the expression

$$\alpha \approx 0.17 \cdot \frac{\lambda}{d} \cdot \mathrm{Re}^{0.33} \cdot \mathrm{Pr}^{0.43} \cdot \mathrm{Gr}^{0.1} \cdot \left(\frac{\mathrm{Pr}}{\mathrm{Pr}_w}\right)^{0.25}. \quad (8)$$

By substituting the value of thermal conductivity λ and the Prandtl number at a temperature of

$$t \approx 26.3\,^{\circ}\mathrm{C}$$

and wall temperature t_w, we obtain

$$\alpha \approx 619\ \mathrm{W}/(\mathrm{m}^2\mathrm{K}).$$

Using Newton's heat transfer equation, we determine the amount of heat flux removed by the water:

$$\alpha \cdot (t_w - t) \cdot S_{Q1} \approx 619 \cdot (38 - 26.3) \cdot 1.39 \approx 10070\ \mathrm{W}.$$

It should be noted that the wetted surface area of the walls removing heat exceeds the frontal wall area due to the presence of longitudinal ribs, i.e.,

$$S_{Qw} > S_{Q1}.$$

Therefore, the natural circulation of water reliably removes the entire heat flux generated by the photovoltaic cells.

Iteration calculations are also carried out for the high-temperature Λ-PM, beginning with an inlet temperature

$$t_{\mathrm{in}2} \approx 45\,^{\circ}\mathrm{C}.$$

As a result, the heat transfer coefficient is found to be

$$\alpha \approx 678\ \mathrm{W}/(\mathrm{m}^2\mathrm{K}).$$

At a flow rate of

$$\dot{m}_2 \approx 690\ \mathrm{kg/h},$$

this provides dissipation of thermal power given by

$$\alpha \cdot (t_w - t) \cdot S_{Q2} \approx 678 \cdot (68 - 54) \cdot 1.54 \approx 14600\ \mathrm{W},$$

which exceeds the peak power generated by the photovoltaic cells.

The water flow rate through the two circulation circuits is determined by the expression

$$\dot{m} \approx (0.3 \cdot \dot{m}_1 + 0.2 \cdot \dot{m}_2),$$

with the inlet water temperature increasing up to approximately 60 upon exiting the storage system.

Thus, the numerical experiment convincingly demonstrates that natural circulation ensures reliable cooling of the photovoltaic cells, allowing them to operate with high efficiency.

Based on the mathematical model of the intensive cogeneration process, a calculation method for a prototype energy complex with larger Maxeon photovoltaic cells has been developed, with their specifications presented in Table 1.

At temperatures $t_{f1} \leq 40^{\circ}\mathrm{C}$ and $t_{f2} \leq 70^{\circ}\mathrm{C}$, the efficiencies of the photovoltaic cells are $\eta_{e1} = 0.20$ and $\eta_{e2} = 0.16$, respectively.

The base number of photovoltaic cells on the channel walls is $n = 100$ units. The area of the low-temperature array is

$$S_{f1} \approx (2n + 10) S_A \approx 1.79\ \mathrm{m}^2,$$

and the high-temperature array is

$$S_{f2} \approx (2n + 34) S_A \approx 1.99\ \mathrm{m}^2.$$

Accordingly, the length of the walls is

$$L_1 = (n + 5) \cdot 0.054 \approx 5.67\ \mathrm{m},$$

$$L_2 = (n + 17) \cdot 0.054 \approx 6.32\ \mathrm{m},$$

with their areas

$$S_{Q1} = 2L_1(b_{f1} + 0.025)$$

$$\approx 5.67 \cdot 0.186 \approx 2.11\ \mathrm{m}^2$$

Table 1 – Specifications of Maxeon Photovoltaic Cells

$S_{Ge5} = 0.167 \times 0.054\,\mathrm{m}$	$S_A = b_f \cdot \frac{S_A}{3} \approx 0.161 \times 0.053\,\mathrm{m}$	
η_{e0}	0.22	0.45
P_0, W	1.95	2.47
V_{mp}, v	0.6	0.78
I_{mp}, A	3.4	3.65
V_{oc}, W	0.64	0.79

Table 2 – Meteorological data for Kazakhstan stations at latitude $\varphi_{\text{IN}} \approx 43^\circ$

Month	1	2	3	4	5	6	7	8	9	10	11	12
τ_M, h	92	91	118	145	171	185	168	168	134	100	87	95
I_m, W/m^2	880	920	950	930	930	940	930	920	920	900	899	850
t_0, °C	-10	-5	10	15	20	35	35	25	15	10	5	-10

$$S_{Q2} = 2L_2(b_{f1} + 0.025) \approx 2.38 \text{ m}^2,$$

where

$$\frac{S_f}{S_Q} \approx 0.85.$$

With $N = 12$ mirrors, the optical aperture area of the energy complex is:

$$A_k \approx 2Nb_z\left[(L_1 + \Delta L) + (L_2 + \Delta L)\right] \cdot \cos\varphi_i^{\text{avg}}/4 \approx 54.7 \text{ m}^2.$$

On the upper walls of the Λ-PM channels, photovoltaic cells are installed that operate with a single concentration of both direct and diffuse radiation $(I_m + I_{\text{dif}})$. Therefore, the total peak electrical power of the prototype is given by:

$$P_c = [7.9I_m + (I_m + I_{\text{dif}})]\left(\eta_{e1}S_{f1} + \eta_{e2}S_{f2}\right) = 5.35I_m + 0.68(I_m + I_{\text{dif}}).$$

The total peak thermal power of the prototype is calculated using the expression:

$$Q_c = S_{Q1}(7.5I_m - 1.5q_{\Lambda 1}) + S_{Q2}(7.7I_m - 1.5q_{\Lambda 2}).$$

As the length of the channels increases, the pressure head also increases, which positively impacts the intensity of cooling for the photovoltaic cells.

The calculation of the performance characteristics of the energy complex prototype with low- and high-temperature Λ-PMs and Maxeon Ge5 photovoltaic cells is carried out using a Python-based software application. The database from the climatic directory [14] is used, which includes average monthly solar radiation intensity on a normal plane I_m, the number of sunshine hours τ_M, and the ambient temperature at the installation site of the prototype.

In Figure 3, the results of the calculation for the average monthly specific electrical and thermal power of the prototype are presented. These results are obtained using the following expressions:

$$\frac{P}{A_k} \approx 0.107I_m,$$

and

$$\frac{Q}{A_k} = \frac{34I_m - 3.16q_{\Lambda 1} - 3.57q_{\Lambda 2}}{54.7}.$$

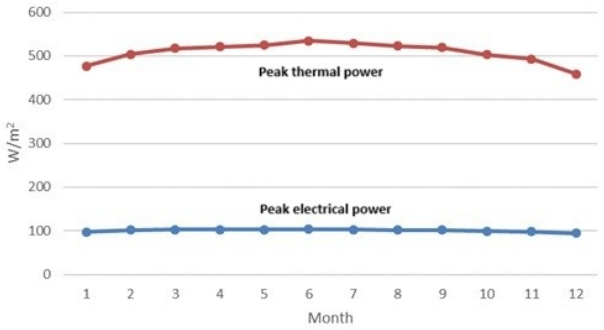

Figure 3 - Specific peak electrical and thermal power of the prototype

Note that in conditions with poorer solar resources, the energy complex prototype has a higher specific power for both electricity and heat compared to the Cogenra Solar system, which, at a ninefold concentration of sunlight at the latitude of South Carolina (≈ 35°N), has peak specific powers of approximately 100 W/m^2 for electricity and 498 W/m^2 for heat.

Using the data from Table 2 on the number of sunshine hours τ_M, we calculate the average monthly performance of the prototype:

$$W_P = \tau_M \cdot \frac{P}{A_k},$$

and

$$W_Q = \tau_M \cdot \frac{Q}{A_k}.$$

Graphs of these calculations are shown in Figure 4.

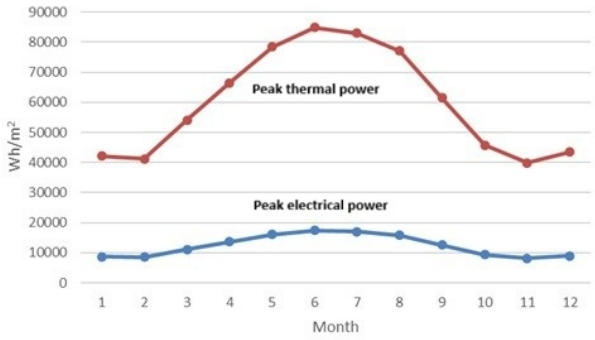

Figure 4 - Specific performance of adjacent Λ-PMs

Summing up the monthly performance, we find the annual specific performance for electricity:

$$\sum W_P \approx 148 \text{ kWh/m}^2,$$

and for heat:

$$W_Q \approx 717 \text{ kWh/m}^2,$$

with an outlet water temperature of approximately 60°C in the storage system.

In comparison, the Cogenra Solar system had a performance of approximately 168 kWh/m^2 and approximately 657 kWh/m^2 with the same outlet temperature of the heat carrier at a latitude with higher solar resources, both in terms of solar intensity and the number of sunshine hours per day.

Figure 5 illustrates the values for the flow rate of hot water at an approximate temperature of 60°C. According to GOST standards, the standard hot water consumption per person is approximately 100 liters per day. Thus, the average flow rate of 270 kg/h provided by the prototype meets the needs of an average farming family for hot water supply, considering household activities.

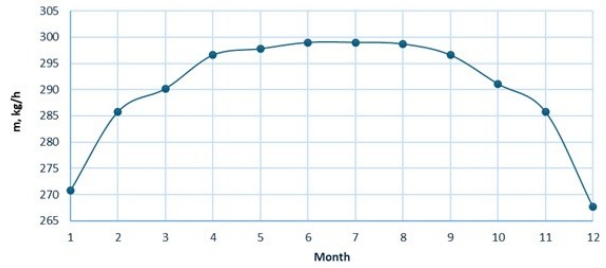

Figure 5 - Hot water flow rate at temperature ≈ 60°C

The technology of intensive cogeneration has the potential to enhance key indicators through improvements in the design of the Λ-PM and the performance of photovoltaic elements [15], which will reduce the payback period of capital investments to four years. The possibility of reducing the payback time of investments is achievable through the implementation of business products derived from the energy complex's working environment.

Conclusions

1. The fundamentally new design of the Λ-PM, with counter-mounted front walls of opposite channels, reduces their weight and optical losses by approximately 4%, decreases thermal losses from radiation and convection by about 27%, and allows for the effective use of silicon photovoltaic elements in heating water to the temperature level required for consumer hot water supply.

2. The integrated operation of low- and high-temperature Λ-PM units with a common storage capacity eliminates the internal contradiction of cogeneration technology caused by the decrease in photovoltaic efficiency. It achieves stabilization of the photovoltaic elements' temperature at approximately 40°C and 70°C, while water with a temperature of approximately 60°C is transported to the storage system without the use of circulation pumps.

3. The process of direct conversion of the heat emitted by photovoltaic elements into work for lifting water is based on a unique combination of the rate of change in density

and viscosity within the operating temperature range, which stabilizes natural circulation through the thermosiphon effect (know-how).

4. Computer simulation results using software applications show that the specific peak power of an autonomous energy complex with low- and high-temperature Λ-PM units exceeds the specific peak power of the known Cogenra Solar installation by SunPower.

5. The integration of low- and high-temperature Λ-PM units within a single supporting structure creates a synergistic effect, manifested in increased performance, elimination of energy costs for pumps, and the use of high-potential thermal energy at the point of generation for technological applications.

6. The innovative cooling system enhances the efficiency of photovoltaic elements and meets the energy consumption standards of a farming family, including hot water supply.

Author Contributions: Conceptualization, P.Nesterenkov and L.Nesterenkova; methodology, P.Nesterenkov, A.Temirbekov and S.Starukhin; software, P.Nesterenkov and A.Nesterenkov; validation, S.Starukhin; formal analysis, L.Nesterenkova; investigation, P.Nesterenkov and L.Nesterenkova; resources, A.Nesterenkov; data curation, A.Nesterenkov; writingoriginal draft preparation, P.Nesterenkov, A.Temirbekov and L.Nesterenkova; writingreview and editing, P.Nesterenkov; visualization, P.Nesterenkov; supervision, A.Temirbekov; project administration, P.Nesterenkov. All authors have read and agreed to the published version of the manuscript.

REFERENCES

[1] Zimmermann, S., H. Helmers, M. K. Tiwari, S. Paredes, B. Michel, M. Wiesenfarth, A. W. Bett, and D. Poulikakos. “A high-efficiency hybrid-concentration photovoltaic system.” *International Journal of Heat and Mass Transfer* 89 (2015): 514–521.

[2] Echer, W., R. Ghannam, A. Kahlil, S. Paredes, and B. Michel, “Advanced liquid cooling for concentrated photovoltaic electro-thermal co-generation.” in *3rd International Conference on Thermal Issues in Emerging Technologies (ThETA 3)*, Cairo, Egypt, 2010, dec. 19–22.

[3] Cogenra Solar Inc., “Cogenra solar installation guide.” accessed February 15, 2024.

[4] Stylianou, S., “Thermal simulation of low concentration pv/thermal system using a computational fluid dynamics software.” Master’s thesis, Delft University of Technology, 2016, master’s Thesis, August 30.

[5] Coventry, J. S. “Performance of a concentrating photovoltaic/thermal solar collector.” *Solar Energy* 178 (2005): 211–222.

[6] Ji, X., M. Li, W. Lin, L. Wang, and X. Luo. “Modeling and characteristic parameter analysis of a trough concentrating photovoltaic/thermal system with gaas and super cell arrays.” *International Journal of Photoenergy* 2012 (2012): 1–10.

[7] Bernardo, L. R., B. Perers, H. Hakansson, and B. Karlsson. “Performance evaluation of concentrating photovoltaic/thermal systems: A case study from sweden.” *Solar Energy* 85 (2011): 1499–1510.

[8] Abdulina, Z., Y. Yerdesh, A. Toleukhanov, M. Mohanraj, A. Rattner, and Y. Belyayev. “Solar-assisted auto-cascade heat pump for water heating in the continental climates.” *International Journal of Mathematics and Physics* 16, no. 2 (2025): 54–63.

[9] Yerdesh, Y., Y. Belyayev, and M. Baiseitov, D.and Murugesan. “Modeling two-phase flow in pipe of the solar collector.” *International Journal of Mathematics and Physics* 9, no. 1 (2018): 1219.

[10] Baitureyeva, A. and B. Rysbaiuly. “Inverse problem for determining the coefficient in the heat conduction equation.” *International Journal of Mathematics and Physics* 15, no. 2 (2024): 101–109.

[11] Luque, A. *Solar Cells and Optics for Photovoltaic Concentration*. California: University of California, 2008.

[12] Bonilla, C., Ed. *Heat Transfer Issues in Nuclear Engineering*. Moscow: Gosatomizdat, 1961.

[13] Mikheev, M. A. and I. M. Mikheeva. *Fundamentals of Heat Transfer*. Moscow: Energia, 1973.

[14] *Climate Reference Book of the USSR. Series 3. Long-Term Data, Parts 1–6, Vol. 18, Kazakh SSR, Book 1*. Hydrometeoizdat, 1989.

[15] Nesterenkov, P. A., A. G. Nesterenkov, and A. N. Temirbekov. "Cogeneration plants with solar radiation concentrators." *Thermal Engineering* 67, no. 10 (2020): 706–714.

Information about authors

Nesterenkov Peter *– M.Sc., Al-Farabi Kazakh National University, Almaty, Kazakhstan, e-mail:stolkner@gmail.com*
Nesterenkova Laryssa *– PhD, Assistant Professor, Al-Farabi Kazakh National University, Almaty, Kazakhstan, e-mail:nesnerenkova@gmail.com*
Temirbekov Almas *– PhD, Al-Farabi Kazakh National University, Almaty, Kazakhstan, e-mail: Almas.Temirbekov@kaznu.kz*
Nesterenkov Arthur *– Al-Farabi Kazakh National University, Almaty, Kazakhstan, e-mail: stolknerphone@gmail.com*
Starukhin Sergey *– Al-Farabi Kazakh National University, Almaty, Kazakhstan, e-mail: ionotexnica@mail.ru*